The Journal of GIS Association of Korea, Vol. 15, No. 4, pp. 397-406, December 2007

2D Flood Simulation for Estimating the Economic Loss in the Building Areas

Sang Hyeok Kang*

ABSTRACT

2D hydraulic models of urban areas are at the forefront of current research of flood inundation mechanisms, but they are constrained by inadequate parameters of topography and insufficient data. In this paper a numerical model based on DEMs is presented to represent overflow waters due to bank break in urban areas. The surface flow in the building areas is assumed to be properly modeled by solving Saint-Venant equation. In order to represent flooding broken out in Samcheok city, 2002, hydraulic model test using tracer has been carried out and validated. These efforts will serve for making flood hazard map and for estimating economic loss due to inundation of personal properties in urban areas.

Keywords : Hydraulic tracer test, 2-dimension, urban flood model, inundation depth

요 약

도시지역의 2차원 모형은 홍수침수과정에 있어서 아직 선구적인 분야이며 이러한 모형은 지형 및 불충분한 지형계수 및 자료로 인하여 제한적으로 이용되고 있다. 본 연구에서는 도시지역의 DEM에 기초한 제방 붕괴로 인한 표면수의 침수를 재현하고자 한다. 도시지역에 있어서 표면수의 흐름은 Saint-Venant의 방정식을 통해 모형을 구성하였다. 2002년 삼척시에서 발생한 홍수를 재현하기 위하여 추적자를 이용한 수리모형실험을 수행하여 모형을 보정하였다. 본 연구는 향후 홍수지도 제작이나 도시지역에서 침수에 따른 경제적 손실을 평가하는데 유용하게 이용될 것이다.

주요어 : 수리학적 추적자, 2차원, 도시홍수모형, 침수심

* Research & Development Institute of Halla Eng. & Construction Corp. (kang7231@hanmail.net)

1. Introduction

Floods are among the most frequent and costly natural disasters in terms of human hardship and economic loss. As much as 70 percent of the damage related to all natural disasters in Korea is caused by water-related disaster and associated debris flows (Kang, 2003). The study of flood phenomenon is of great complexity. Many studies have been carried out in the past to represent inundation depth and velocity in urban areas (Inoue et al. 1999; Noguchi et al. 1992; 1994; Takeda et al., 2003). But these models consider only surface and river flows. Compared to rural areas, it is more difficult to simulate flooding in urban areas due to the presence of small-scale system feature like roads, buildings, and dykes that block and affect flooding inundation. Commonly large Digital Elevation Models (DEMs) grid elements make up the model domain in order to reduce the computation time (Dutta, 1999; Hosoyamada, 2005). This allows for quick model calibrations and sensitivity analysis but also, in operational mode, it allows flood forecasting in real time. A major disadvantage of the use of low resolution input data is the loss of important small-scale features that affect flood propagation. As such there is a need to quantify the effects such averaging has on model performance and, more importantly, the reliability of simulation results.

Horritt et al. (2001; 2002) evaluated the flood simulation results obtained from a 1D raster based model and a 2D model. The results indicated that simulated topographic properties had a major effect on simulation results and that topography is a major factor in determining flood inundation patterns.

The major issue in high-density urban areas is obtaining accurate input data for the model. We integrated an urban flood model and described a data processing procedure to estimate the influence of building and DEMs size. GIS was used to perform the pre- and post-processing of large amounts of spatial input and output data results efficiently.

2. Model structure

2.1 Rainfall-runoff

The runoff analysis from watershed includes both slope and mountainous river flow. The governing equations based on the kinematic wave model are as follows:

For slope flow

$$\frac{\partial h}{\partial t}+\frac{\partial q}{\partial x}=r_e \tag{1}$$

$$q=\alpha h^m \tag{2}$$

where x is a one-dimensional spatial coordinate; t is time; q is discharge per unit width on the slope; r_e is effective rainfall; h is water depth; a and m are constants, respectively (m'=5/3; $a=\sqrt{\sin\theta}/N$; θ, slope gradient; N, equivalent roughness according to Manning's law).

For river flow

$$\frac{\partial h}{\partial t}+\frac{\partial q'}{\partial x}=\frac{q_s}{B} \quad (3)$$

$$q'=\alpha h^{m'} \quad (4)$$

where q' is discharge per unit width on the mountainous river; q_s is lateral inflow per unit width from the slope; B is mountainous river width; α and m' are constants ($\alpha=\sqrt{\sin\theta_r}/n$; θ_r, river bed slope; n, roughness coefficient; m'=5/3).

The lateral inflow from the slope of the river is calculated by the characteristics method and the runoff discharge along the river is calculated by the finite different method using the Leap-Frog method (Kawaike et al, 2000).

2.2 Sewer system

The rainwater in the sewer pipe is calculated on the following continuity and momentum equations;

$$\frac{\partial A}{\partial t}+\frac{\partial Q}{\partial x}=q \quad (5)$$

$$\frac{\partial Q}{\partial t}+\frac{\partial (uQ)}{\partial x}=gA\frac{\partial H}{\partial x}-\frac{gn^2|Q|Q}{R^{4/3}A} \quad (6)$$

where A is cross sectional area of flow; Q is discharge; q is later inflow; u is flow velocity; H is water level ($H=h+z$); z is elevation of sewer pipe from bottom; h is calculated as:

$$h=\begin{Bmatrix}\frac{A}{B}:(A<A_p)\\ B'+\frac{A-A_p}{B_s}:(A>A_p)\end{Bmatrix} \quad (7)$$

where B is pipe width; A_p is cross sectional area of pipe; B' is height of pipe ceiling; B_s is slot width.

2.3 Urban area

Governing equations for 2D varied unsteady flow can be derived from mass conservation and momentum equations. Overland flow equations are the 2D expansion of St. Venant's 1D open channel flow equations as follow:

For continuity equation (mass conservation equation)

$$\frac{\partial h}{\partial t}+\frac{\partial M}{\partial x}+\frac{\partial M}{\partial y}=0 \quad (8)$$

For momentum equations

$$\frac{\partial M}{\partial t}+\frac{\partial (uM)}{\partial x}+\frac{\partial (vM)}{\partial y}=-gh\frac{\partial H}{\partial x}-\frac{\tau_{bx}}{\rho_w} \quad (9)$$

$$\frac{\partial N}{\partial t}+\frac{\partial (uN)}{\partial x}+\frac{\partial (vN)}{\partial y}=-gh\frac{\partial H}{\partial y}-\frac{\tau_{by}}{\rho_w} \quad (10)$$

where h is water depth; u and v are velocities of flow in x and y direction; M and N are fluxes of discharge in x and y directions ($M=uh$, $N=vh$); H is water level written as $H=h+z$ (z is elevation). τ_{bx} and τ_{by} are x and y components of shear stress on the water bottom as follows:

$$\tau_{bx}=\frac{\rho_w g n^2 u\sqrt{u^2+v^2}}{h^{1/3}} \quad (11)$$

$$\tau_{by}=\frac{\rho_w g n^2 v\sqrt{u^2+v^2}}{h^{1/3}} \quad (12)$$

where ρ_w is water density; g is gravity acceleration; n is Manning's roughness.

Solving the Saint-Venant equations

If we assume that i and j are the number of grid and upper n is time step, the Eq. (8) can be written as:

$$\frac{h_{i,j}^{n+3}-h_{i,j}^{n+1}}{2\Delta t}+\frac{M_{i+1/2,j}^{n+2}-M_{i-1/2,j}^{n+2}}{\Delta x}+\frac{N_{i,j+1/2}^{n+2}-N_{i,j-1/2}^{n+2}}{\Delta y}=0 \tag{13}$$

For x-component momentum equation

$$\begin{aligned}
&\frac{M_{i-1/2,j}^{n+2}-M_{i-1/2,j}^{n}}{2\Delta t}\\
&+\frac{u_{i,j}^{n}\dfrac{M_{i-1/2,j}^{n}+M_{i+1/2,j}^{n}}{2}+\left|u_{i,j}^{n}\right|\dfrac{M_{i-1/2,j}^{n}-M_{i+1/2,j}^{n}}{2}}{\Delta x}\\
&-\frac{u_{i-1,j}^{n}\dfrac{M_{i-3/2,j}^{n}+M_{i-1/2,j}^{n}}{2}+\left|u_{i-1,j}^{n}\right|\dfrac{M_{i-3/2,j}^{n}-M_{i-1/2,j}^{n}}{2}}{\Delta x}\\
&+\frac{v_{i-1/2,j+1/2}^{n}\dfrac{M_{i-1/2,j}^{n}+M_{i-1/2,j+1}^{n}}{2}+\left|v_{i-1/2,j+1/2}^{n}\right|\dfrac{M_{i-1/2,j}^{n}-M_{i-1/2,j+1}^{n}}{2}}{\Delta y}\\
&-\frac{v_{i-1/2,j-1/2}^{n}\dfrac{M_{i-1/2,j-1}^{n}+M_{i-1/2,j}^{n}}{2}+\left|v_{i-1/2,j-1/2}^{n}\right|\dfrac{M_{i-1/2,j-1}^{n}-M_{i-1/2,j}^{n}}{2}}{\Delta y}\\
&=-g\frac{h_{i,j}^{n+1}+h_{i-1,j}^{n+1}}{2}\cdot\frac{(h_{i,j}^{n+1}+z_{i,j})-(h_{i-1,j}^{n+1}+z_{i-1,j})}{\Delta x}\\
&-\frac{g\left(\dfrac{n_{i,j}-n_{i-1,j}}{2}\right)^{2}\dfrac{M_{i-1/2,j}^{n+2}+M_{i-1/2,j}^{n}}{h_{i,j}^{n+1}+h_{i-1,j}^{n+1}}\sqrt{\left(u_{i-1/2,j}^{n}\right)^{2}+\left(v_{i-1/2,j}^{n}\right)^{2}}}{\left(\dfrac{h_{i,j}^{n+1}+h_{i-1,j}^{n+1}}{2}\right)^{1/3}}
\end{aligned} \tag{14}$$

For y-component momentum equation

$$\frac{N_{i,j-1/2}^{n+2}-n_{i,j-1/2}^{n}}{2\Delta t}$$

$$\begin{aligned}
&+\frac{u_{i,j}^{n}\dfrac{N_{i,j-1/2}^{n}+N_{i+1,j-1/2}^{n}}{2}+\left|u_{i,j}^{n}\right|\dfrac{N_{i,j-1/2}^{n}-N_{i+1,j-1/2}^{n}}{2}}{\Delta x}\\
&-\frac{u_{i-1/2,j-1/2}^{n}\dfrac{N_{i-1,j-1/2}^{n}+N_{i,j-1/2}^{n}}{2}+\left|u_{i-1/2,j-1/2}^{n}\right|\dfrac{N_{i-1,j-1/2}^{n}-N_{i,j-1/2}^{n}}{2}}{\Delta x}\\
&+\frac{v_{i,j}^{n}\dfrac{N_{i,j-1/2}^{n}+N_{i,j+1/2}^{n}}{2}+\left|v_{i,j}^{n}\right|\dfrac{N_{i,j-1/2}^{n}-N_{i,j+1/2}^{n}}{2}}{\Delta y}\\
&-\frac{v_{i,j-1}^{n}\dfrac{N_{i,j-3/2}^{n}+N_{i,j-1/2}^{n}}{2}+\left|v_{i,j-1}^{n}\right|\dfrac{N_{i,j-3/2}^{n}-N_{i,j-1/2}^{n}}{2}}{\Delta y}\\
&=-g\frac{h_{i,j}^{n+1}+h_{i,j-1}^{n+1}}{2}\cdot\frac{(h_{i,j}^{n+1}+z_{i,j})-(h_{i,j-1}^{n+1}+z_{i,j-1})}{\Delta y}\\
&-\frac{g\left(\dfrac{n_{i,j}-n_{i,j-1}}{2}\right)^{2}\dfrac{N_{i,j-1/2}^{n+2}+N_{i,j-1/2}^{n}}{h_{i,j}^{n+1}+h_{i,j-1}^{n+1}}\sqrt{\left(u_{i,j-1/2}^{n}\right)^{2}+\left(v_{i,j-1/2}^{n}\right)^{2}}}{\left(\dfrac{h_{i,j}^{n+1}+h_{i,j-1}^{n+1}}{2}\right)^{1/3}}
\end{aligned} \tag{15}$$

where,

$$u_{i-1/2,j}^{n}=\frac{2M_{i-1/2,j}^{n}}{h_{i,j}^{n+1}+h_{i-1,j}^{n+1}},v_{i,j-1/2}^{n}=\frac{2N_{i,j-1/2}^{n}}{h_{i,j}^{n+1}+h_{i,j-1}^{n+1}} \tag{16}$$

$$u_{i,j-1/2}^{n}=\frac{u_{i-1/2,j}^{n}+u_{i+1/2,j}^{n}+u_{i-1/2,j-1}^{n}+u_{i+1/2,j-1}^{n}}{4} \tag{17}$$

$$v_{i-1/2,j}^{n}=\frac{v_{i,j-1/2}^{n}+v_{i-1,j-1/2}^{n}+v_{i,j+1/2}^{n}+v_{i-1/2,j+1/2}^{n}}{4} \tag{18}$$

$$u_{i,j}^{n}=\frac{u_{i-1/2,j}^{n}+u_{i+1/2,j}^{n}}{2},u_{i-1,j}^{n}=\frac{u_{i-3/2,j}^{n}+u_{i-1/2,j}^{n}}{2} \tag{19}$$

$$v_{i,j}^{n}=\frac{v_{i,j-1/2}^{n}+v_{i,j+1/2}^{n}}{2},v_{i,j-1}^{n}=\frac{v_{i,j-3/2}^{n}+v_{i,j-1/2}^{n}}{2} \tag{20}$$

$$u_{i+1/2,j-1/2}^{n}=\frac{u_{i+1/2,j}^{n}+u_{i+1/2,j-1}^{n}}{2},u_{i-1/2,j-1/2}^{n}=\frac{u_{i-1/2,j}^{n}+u_{i-1/2,j-1}^{n}}{2} \tag{21}$$

$$v_{i-1/2,j+1/2}^{n}=\frac{v_{i,j+1/2}^{n}+v_{i-1,j+1/2}^{n}}{2},v_{i-1/2,j-1/2}^{n}=\frac{v_{i,j-1/2}^{n}+v_{i-1,j-1/2}^{n}}{2} \tag{22}$$

3. Model verification

The model was verified using tracer in the Hydraulic Research Laboratory of Disaster Prevention Research Institute, Kyoto University. The scale of hydraulic experimental model is 1:100 as shown in Figure 1. The major purpose was to analyze surface water movement including amount of discharge from inlet pipe into sewer system. The discharge at all inlet pipes was measured using weirs or buckets. The surface water flow in test area was visualized by a tracer method with video cameras as shown in Figure 2 and Figure 3. If there are non-linear areas due to the difference of elevation, the discharge flux, M_0 flows by drop-water (see Figure 4-a) and over-flow (see Figure 4-b) as:

For drop-water

$$M_0 = \mu h_h \sqrt{g h_h} \tag{23}$$

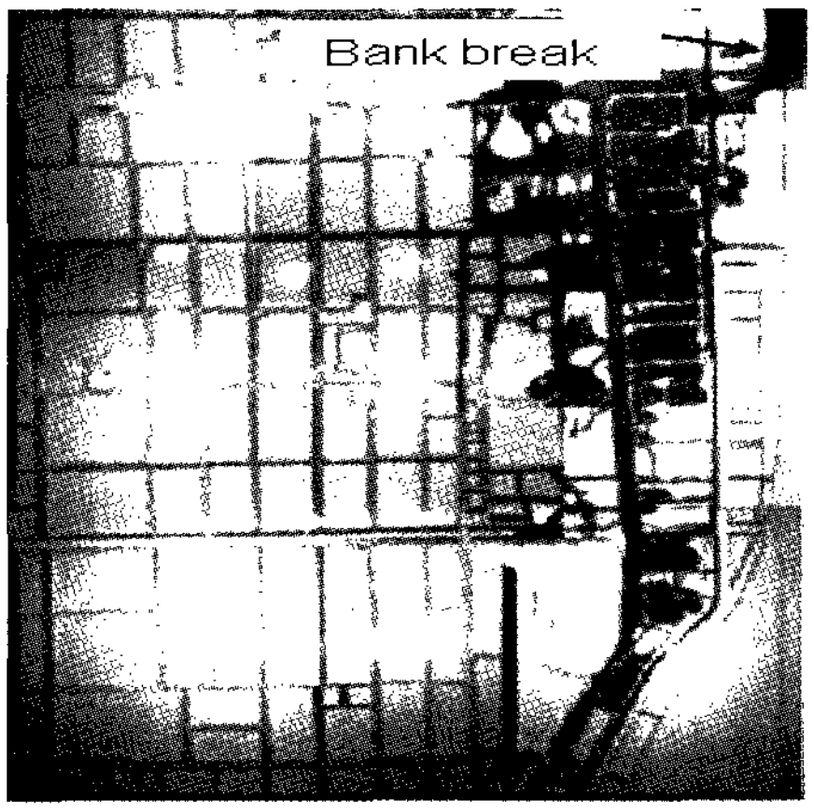

Figure 2. Results of hydraulic model test (T=0.5h later)

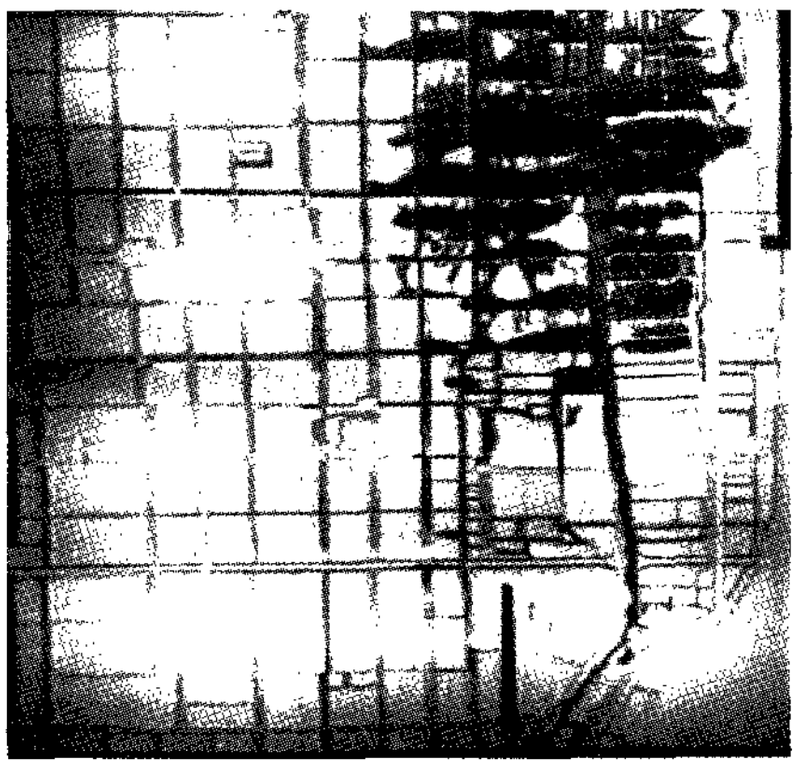

Figure 3. Results of hydraulic model test (T=1.5h later)

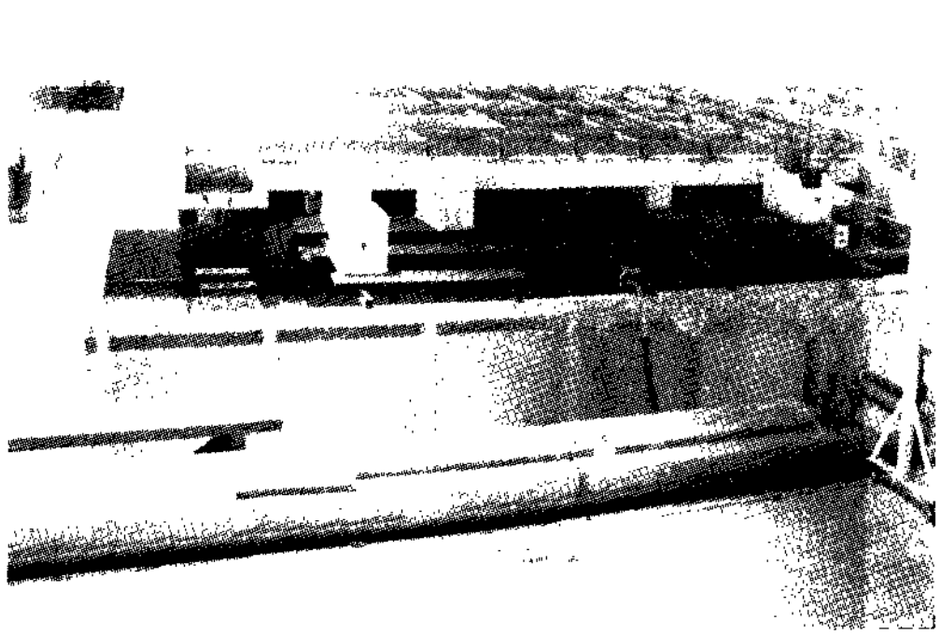

Figure 1. View of hydraulic model test

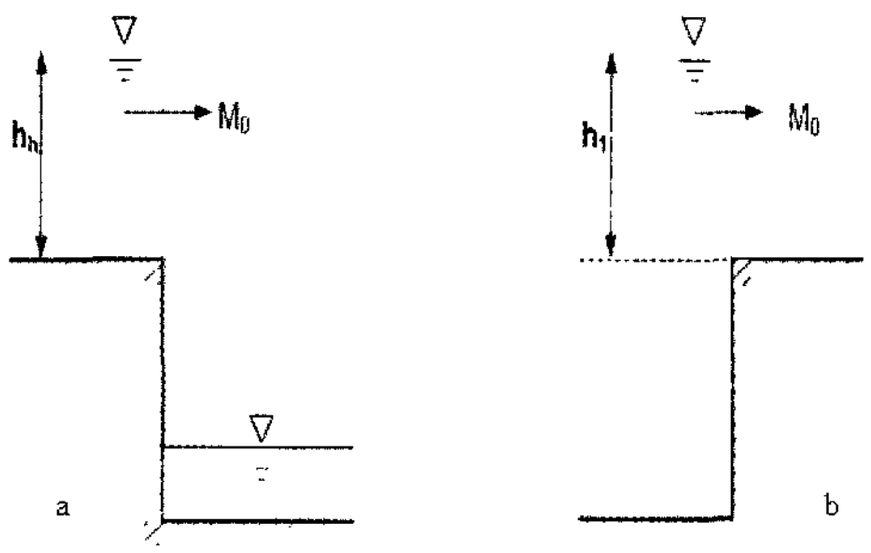

Figure 4. The forehead of overflow waters: (a) for drop-waters; (b) for over-topping waters

Based on the hydraulic model test, discharge coefficient, μ is estimated to be $\mu=(2/3)^{3/2}$; h_h is water depth where the elevation is the highest.

For over-topping water

$$M_0 = \mu' h_1 \sqrt{g h_1} \tag{24}$$

where μ' is discharge coefficient estimated as $\mu'=0.35$; h_1 is water depth where the elevation is the lowest. The river bed material used for the construction was represented by Manning's friction coefficient $n=0.0215\ sm^{-1/3}$ The critical depth for moving waters is given to be 0.001 m.

4. Application to real case and discussion

4.1 Influence of buildings

In order to simulate urban flooding, the influence of buildings should be carefully specified according to the needs of applications. GIS-based hydrological modeling is applied to delineate the basic hydrological elements from a DEMs.

In order to estimate the effect of a building, the share of the building, λ in each grid and the transmissivity of the building, β are applied (Kawaike et al., 2001; Ohtsubo et al., 2001).

$$M^* = \beta M \ , \ N^* = \beta N \tag{25}$$

where M^* and N^* are the flux of discharge which are corrected boundary conditions in x and y components per unit width, respectively. If we consider M^*, N^* and λ, the continuity equation can be written as:

$$(1-\lambda)\frac{\partial h}{\partial t}+\frac{\partial M^*}{\partial x}+\frac{\partial N^*}{\partial y}=r_e-q_{out}+q_{over} \tag{26}$$

where u, v; x, y are components of flow velocity, respectively; $M^*=\beta m$, $N^*=\beta n$, x, y components of corrected discharge per unit width; M, N; x, y components per unit width, respectively; q_{out}, drainage discharge per unit area from the computational mesh into the sewer system; q_{over}, overtopping discharge flow per unit area of the computational grid from the river network.

If we assume that i and j are the number of grid and upper n is time step, the Eq. (26) can be written as:

$$(1-\lambda_{i,j})\frac{h_{i,j}^{n+3}-h_{i,j}^{n+1}}{2\Delta t}+\frac{M_{i+1/2,j}^{*n+2}-M_{i-1/2,j}^{*n+2}}{\Delta x}$$
$$+\frac{N_{i,j+1/2}^{*n+2}-N_{i,j-1/2}^{*n+2}}{\Delta y}=r_e-q_{out}+q_{over} \tag{27}$$

The possible representations of buildings for the model are illustrated in Figure 5. The buildings are represented as solid objects. In order to extract building properties, GIS techniques were applied as shown in Figure 6. In real world, the propagation of flood is decreased due to buildings' influence. If the number of buildings is decreased in the areas of flood, than the inundation depth will be increased. The data of building areas are converted into an image which is converted into

a polygon using a geo-concept image. For extracting buildings, a minimum filter method by Arc-info was used.

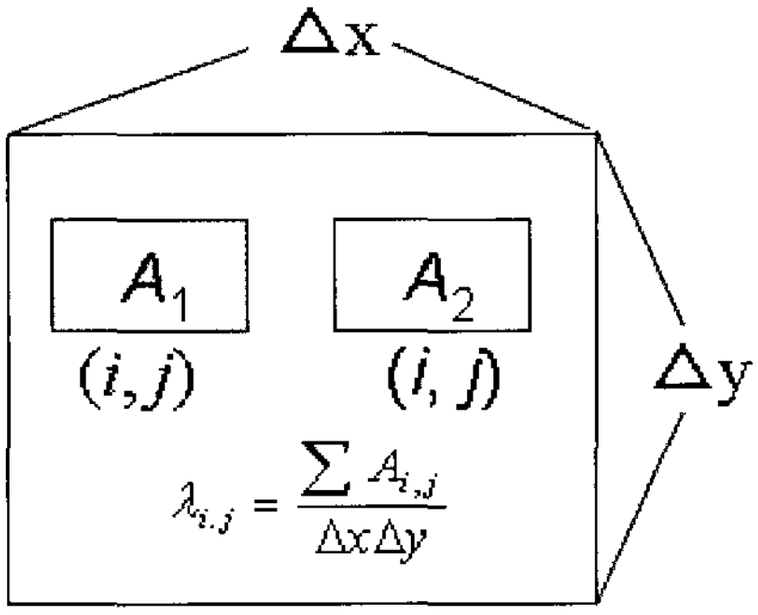

Figure 5. Concept of building' s sharing (A_1) and (A_2) in each grid

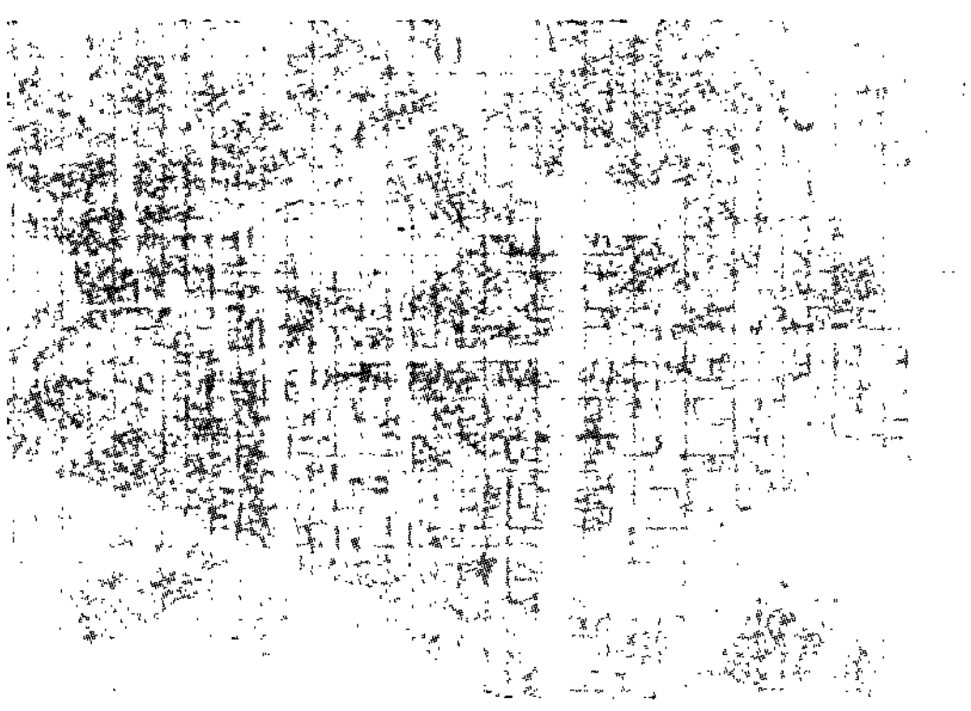

Figure 6. Overlay of buildings per the grid for extraction of building areas

4.2 Influence of DEMs size with building

In the real world topography is one of the critical factors affecting the propagation of a flood wave in urban areas. Clearly, geometrical properties of topography may obstruct the flow but also could conduct or accelerate the flow of water. In hydraulic modeling, the results of output are affected to a large extent by model input data such as DEMs and related properties of slope gradients, slope aspects and drainage density. Understanding the relationships between flow depth, velocity and inundation area across the model domain is of great interest in modeling but difficult to define. Often there is a dilemma of selecting an appropriate DEMs size. The DEMs size should be selected in such way that computational time is acceptable. Since the same water level hydrograph is introduced for the boundary condition of broken point on the dyke, the equal volumes of water are expected to be stored in the model domain. Even if domain areas increase with increased element size, it is assumed that such effect can be ignored, since inflow and outflow boundary elements are of equal size. This is to satisfy the law of mass conservation: for a certain time period, the inflow minus the outflow must be equal to the change in storage.

4.3 Flood flow simulation

The study area to prove the proposed model is Samcheok city, Kangwon province, Republic of Korea. The Samcheok city is surrounded by mountainous areas, and the biggest part of the city consists of low-lying land as shown in Figure 7. The city has a well known history of floods due to heavy rainfall in the past. Annual mean precipitation in the study basin was 1,350, and over 80% of the annual mean rainfall in the basin of study area was con-

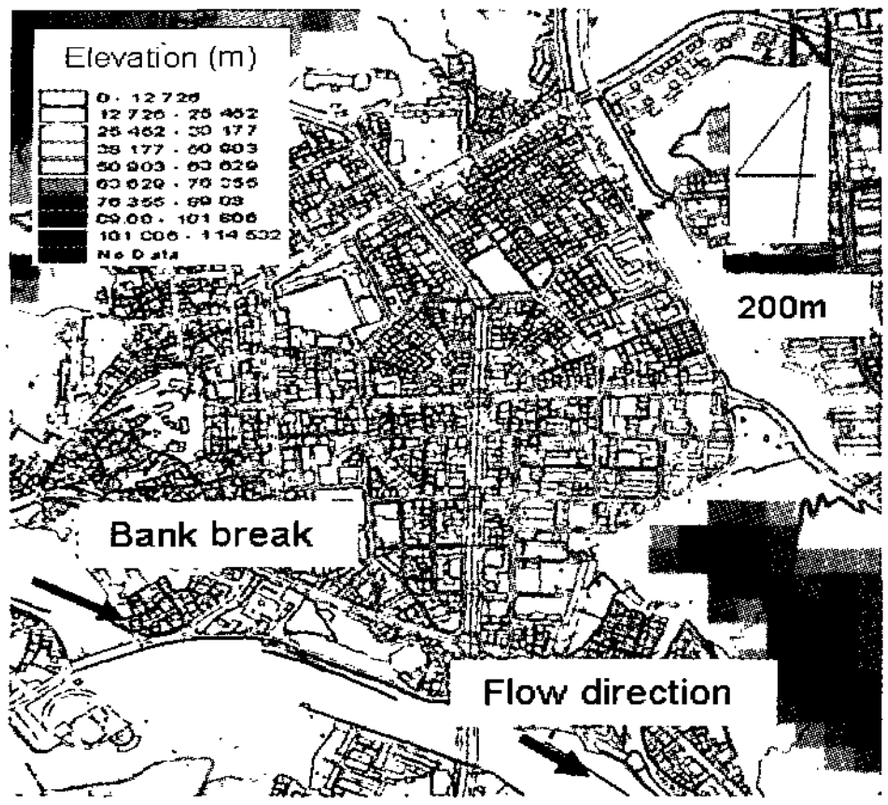

Figure 7. Schematic representation of study areas

centrated in heavy showers occurring several times during rainy season from May to September during 1965-2003 (http://www.wamis.go.kr/). Among them, from August 31st to September 1st 2002, the basin suffered from a large flood due to heavy rainfall caused by typhoon No. 14. The typhoon brought heavy rain of over 700 mm, having inundated 3,639 houses, 200 ha of farmland, and claimed the lives of 13 people. To worsen the matter, another typhoon hit the same region in 2002 resulting in serious damage. The successive disasters gave us an unforgettable experience with people isolated from other town, the paralyzed public and personal infrastructures, wide-spread destruction of property and large human casualties. "*From flood control to flood management*" was a significant milestone and inevitable trend for the adjustment of water management strategies in rapidly developing Korea. The proposed urban model was applied to simulate this flood event. The flooding simulation has been focused on the dyke break which took place in the study period. Figure 8 shows the simulated flood depth for the time when the river dyke just broken out at 19:00 August 31st 2002.

Figure 8. Simulated result 19h later (at just bank break)

Figure 9 shows the simulated maximum flood depth during study period. The upstream boun-

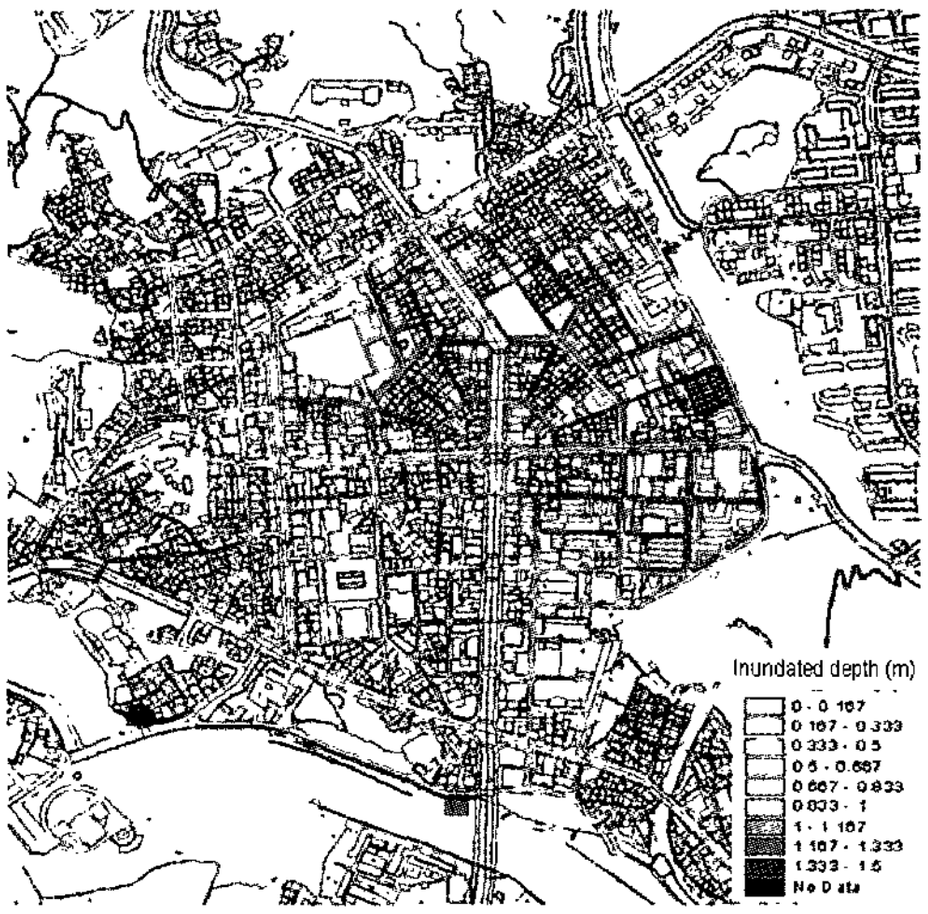

Figure 9. Simulated results at maximum inundated depth

dary condition is provided through a flow boundary in terms of a water level hydrograph. Most of the inundated areas are concentrated in the low elevation region. The flood in inland areas flows and propagates to low-elevation grid quickly.

5. Conclusions

A 2D numerical model has been presented as a tool to simulate shallow water depth in high density building area. Recently, developing computer techniques associated with the greater availability of terrain data in digital form has favored the production of urban flood models, which have spatial variability of topography built into their structures. The availability of digital geographical data, particularly DEMs, gives us new opportunities for using the 2D flow of building areas in the urban planning. Hydraulic models for predicting water surface profiles may be used by local emergency management, public works, planning, flood management, and public safety personal to identify at-risk structures and organizations. The models also provide a basis for predicting the area to be impacted, the water level, and flow extent (corresponding to water surface profiles from selected flows and or high water elevations). The most convenient and user-friendly method to display and query this information is through the use of a GIS. Base map information including an aerial photograph or digital map and point features for critical structures may be used as a backdrop for inundation maps. Each different inundation map may be a separate layer in the GIS. The advantages of the digital data for building areas are rapid collection and the ability to turn accurate digital data into a model. It was demonstrated that urban flood inundation is directly affected by even quite small changes in topography and the model sensitivity using buildings effect was more complex than might have been expected.

Although most of data are inputted in digital form, some like inlets are not available. If they are prepared as digital form, we can save simulation time and the effort required to input the data into the model.

References

Dutta, D. Herath, S., and Musiake, K., 1999. Distributed hydrological model for flood inundation simulation, Annual Journal of Hydraulic Engineering, JSCE, 43, 25-30

Horritt, M.S. and Bates, P. D., 2001. Effects of spatial resolution on a raster based model of flood flow, Journal of Hydrology, 253 239-249.

Horritt, M.S. and Bates, P. D., 2001. Evaluation of 1D and 2D numerical models for predictiong river flood inundation, Journal of Hydrology, 268 87-99.

Hosoyamada, T., 2005. Numerical analysis of flood around residential area in the Niigata heavy rainfall disaster on 13 July, 2004, Annual Journal of Hydraulic Engineering, 49, 589-594.

Inoue, K., Kawaike, K., and Hayashi, H., 1999. Inundation flow modeling in urban area, Annual

Journal of Hydraulic Engineering, 43, 533-538.

Iwasa, Y., Inoue, K., and Mizutori, M., 1979. Hydraulic analysis of overland flood flows by means of numerical method, Annuls of DPRI, Kyoto Univ., 23(B-2), 305-317.

Kang, S.H., 2003. Study on refuge behavior and its critical inundation depth in low area, Journal of Korean Society of Civil Engineers, 23(B37), 561-565.

Kawaike, K., et al, 2001. Development of inundation flow model in urban area located in law-lying river basin, Annuls of DPRI, Kyoto Univ., 44(B-2), 299-311.

Noguchi, M., et al, 1994. An Early Warning System to Mitigate the Flood Disaster in Urban Areas, Proc. of World Conf. on Natural Disaster Reduction, pp.63-64.

Noguchi, M., et al, 1992. Estimation of Sewer Flows under Inundated Conditions, Proc. of Int'l. Symp. on Urban Stormwater Management, Sydney, pp. 372-377.

Ohtsubo, I., et al, 2001. Study on analysis system for overland flood flow by means of GIS, Annual Journal of Hydraulic Engineering, 45, 877-882.

Kakeda, M., et al, 2003. Analysis of flood of the Shounai river due to the heavy rain in Tokai district, Annual Journal of Hydraulic Engineering, 47, 81-86.